IJISET - International Journal of Innovative Science, Engineering & Technology, Vol. 3 Issue 6, June 2016
ISSN (Online) 2348 – 7968 | Impact Factor (2015) - 4.332
www.ijiset.com

A Sensorless Speed Estimation for Brushed DC Motor at Start-up

Brendan Khoo, Muralindran Mariappan and Ismail Saad

Artificial Intelligence Research Unit, Faculty of Engineering, Universiti Malaysia Sabah,
Kota Kinabalu, Sabah 88400, Malaysia

Abstract

Despite the fast growing implementation of brushless DC motor, the older brushed DC motor is still relevant in many commercial, industrial and hobbyist applications due to low-cost and simplicity. Many brushed DC motor applications require precise speed and position control, thus requiring a sensor feedback. Commonly a separate rotary encoder is required to provide speed and positional feedback to the system with additional cost. Therefore, researchers strive to arrive with better and more accurate sensorless speed and position measurement for brush DC motor. However, researchers neglected the measurement of brushed DC motor during starting which is vital for many day-to-day applications. Hence in this paper, a novel sensorless speed estimation method for brushed DC motor at Starting is presented.

Keywords: *Brushed DC Motor, Sensorless Speed Detection, DC Motor Starting, DC Motor Current Ripple, Artificial Neural Network.*

1. Introduction

Brushed DC motor is one of the oldest yet versatile electrical machine ever created. Brushed DC motor is found in almost every day-to-day machine such as ink jet printers, automated vacuum cleaners, robotic manipulators, DVD drives, electric trains, automotive power windows and battery powered hand-drill although brushless DC motors have swiftly taken over many brushed DC motor applications. Brushed DC motor is still the best choice for many low-cost machines due to its simplicity and cost.

A brushed DC motor is very easy to operate and it does not require an external complex driver to operate because it is self-commutated. Speed control of brushed DC motor is also easy because the voltage-speed characteristic of brushed DC motor is relatively linear. However, knowing the actual speed of the rotor is important in applications which require high precision: ink jet printers and mobile robots. Hence, rotary encoders (hall effect and optical) are mounted to the motor shaft to acquire the actual speed and position of the rotor. Many brushed DC motors come with attached rotary encoder too.

Although rotary encoders can provide very accurate speed feedback, harsh operating environment with corrosive gasses, high temperature, intense mechanical vibration and also electrical surges can drastically reduce their lifespan. Hence with the motivation of cost, simplicity and ruggedness, many different sensorless speed measurement techniques have been proposed for brushed DC motor.

In recent years, many researcher proposed different sensorless methods for brushed DC motor which can be separated into few general techniques: equation modelling [1, 2, 3, 4], kickback voltage transient [5, 6], back electro motive force [7, 8] and ripple current counting [9, 10, 11]. Among these techniques, kickback voltage transient and ripple current counting techniques provide the most accurate brushed DC motor speed estimation. Most of these techniques provided solution in estimating the rotor speed at operating speed and only [9] is able to estimate the rotor speed at starting by removing or altering the winding on one of the rotor slot.

Measuring the rotor speed at starting is crucial in precision applications where the final rotational displacement is determined starting from a stationary rotor. Although the technique in [9] is able to acquire the rotor speed starting from a stationary rotor, it required modification to the winding of the rotor which will affect the torque and overall lifespan of the motor. Thus, this paper will propose a novel method to estimate brushed DC motor speed at starting without any invasive modification.

Artificial Neural Network (ANN) is a machine learning algorithm that has been applied in pattern classification problem. This model is applied because of its capability in parallel processing, learning and decision making ability [12]. ANN can reduce misclassification among the inputs [13]. It can adapt to signals that are corrupted by noise and can solve non- linear function. Neural network is a machine that is designed to model the way in which the brain performs a particular task. The network is usually implemented using electronics components or simulated in software on a digital computer. Fig 1 represents the human biological neurons that is used to represent the ANN [14].

IJISET - International Journal of Innovative Science, Engineering & Technology, Vol. 3 Issue 6, June 2016
ISSN (Online) 2348 – 7968 | Impact Factor (2015) - 4.332
www.ijiset.com

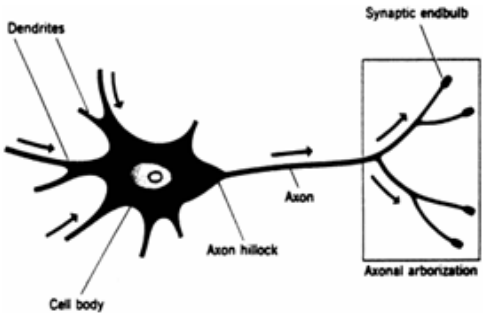

Fig. 1 Biological Neuron

ANN resembles human brain in two aspects:

- Knowledge is acquired by the network through a learning process.
- Interneuron connection strengths known as synaptic weights are used to store the knowledge.

This paper proposed a signal pre-processing and amplification circuit to acquire the brushed DC motor current signal during starting process from stationary. Next, artificial neural network classifier is used to identify the current pulses generated at starting process.

In the following sections, this paper will discuss about the design of the system proposed by the method. The system is then tested with an industrial brushed DC motor. The result of the proposed method is then compared with an optical rotary encoder.

2. Materials and Methods

The proposed method operates on the configuration shown in Fig. 2. The DC machine is a 24V 120watt permanent magnet brushed DC motor. As shown in Fig. 3, a 500 Pulse/Rotation optical encoder is mounted directly to the shaft of the rotor. The driver module consists of a MOSFET H-bridge to control the motor in all four quadrants. The signal conditioning module filters the high-frequency PWM noise and also amplifies the small signal generated from the commutation current. The pre-processed current signal is then digitized at the data acquisition module and transmitted to the computer.

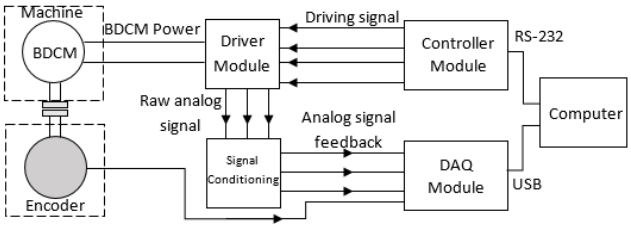

Fig. 2 Proposed beam former

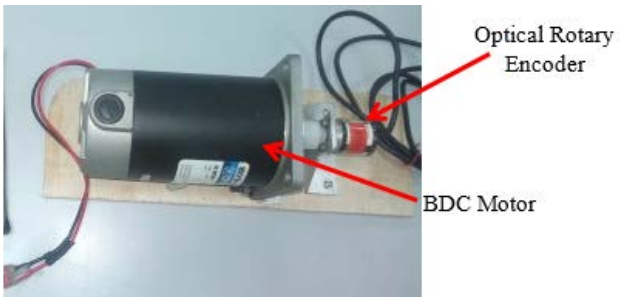

Fig. 3 Motor-Encoder Setup

2.1 Motor Driver and Current Sensing

Fig. 4 shows the brushed DC motor controller designed for this project. It employs full H-bridge for all mode operation (forward, backward, braking and coasting). The H-bridge is constructed with two enhancement mode p-channel MOSFETs and two enhancement mode n-channel MOSFETs. All the selected MOSFETs are high speed and high power HEXFET® for low-loss switching.

The operation mode of the H-bridge is controlled by a low-cost 16-pin microcontroller, PIC16F1827. The microcontroller runs at 5 MIPS or 200 nanoseconds per CPU instruction and provides an accurate on/off timing for each MOSFETs to prevent "shoot through" phenomena which can damage the MOSFETs and the circuit by shorting the +24V rail to the ground. The operation mode can be conveniently controlled by an external controller circuit via two digital input wires to the microcontroller (four states: coasting, reverse, forward and braking).

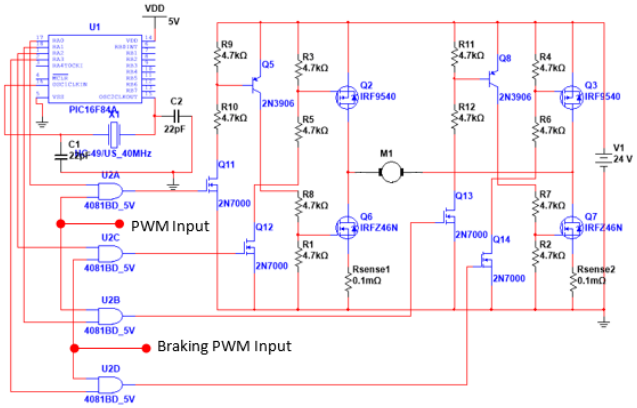

Fig. 4 Brushed DC motor controller

As show in Fig. 4, the speed of the brushed DC motor can be controlled via “PWM Input” which is connected to two CMOS NAND gates. For smoother braking operation, braking strength can be controlled via “Braking PWM Input” shown in Fig. 4.

IJISET - International Journal of Innovative Science, Engineering & Technology, Vol. 3 Issue 6, June 2016
ISSN (Online) 2348 – 7968 | Impact Factor (2015) - 4.332
www.ijiset.com

Finally, the brushed DC motor current can be measured across R_{sense1} and R_{sense2}.

2.2 Signal Pre-amplification

The brushed DC motor current signal sensed across the R_{sense} resistor is dependent on its resistance value. Using Ohm's law, the sensed current signal in the form of voltage difference across is directly proportional to the magnitude of R_{sense}. However, the value of R_{sense} must be maintained at an optimum value. The optimum value of R_{sense} can be determined by maintaining the I^2R value or Ohmic power below the R_{sense} maximum wattage.

The preamplifier circuit in Fig. 5, biases the R_{sense} voltage signal at R_3, R_4 and R_5 to obtain optimum operation range in the TL084. The circuit then performs 21 times amplification on the input signal.

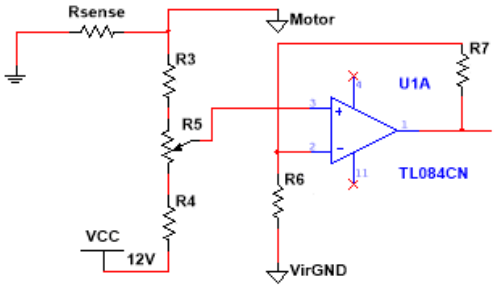

Fig. 5 Preamp circuit

2.3 Signal Filtering and Amplification

The signal filtering and amplification circuit pre-processes the pre-amplified current signal by removing the DC and high-frequency current component and amplifies the important rotor spin-up current signal. This analog circuit acts as a zoom function to capture the region of interest and prevent saturation when high-current starting.

Fig. 6 shows the filter topology for the signal preprocessing module before undergoing digitization by the data acquisition card. The filter topology consists of a second order Sallen-Key high-pass filter which removes the DC voltage offset component and low frequency ac voltage signal that may cause saturation in the amplifiers. The output signal from the high-pass Sallen-Key filter is then passed through a normalization amplifier and amplified to improve the amplitude of the signal.

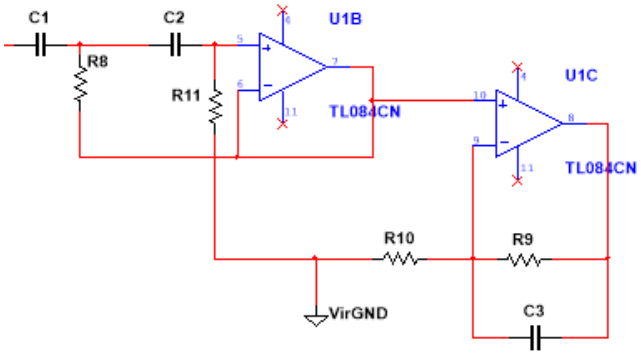

Fig. 6 Signal pre-processing layout

The cut-off frequency f_c of the Sallen-Key high-pass filter can be represented with the equation (1).

$$f_c = \frac{1}{2\pi\sqrt{R_8 C_1 R_{11} C_2}} \quad (1)$$

The transfer function of the Sallen-Key topology is shown in equation (2). Where, V_O denotes output voltage, V_I is the input voltage, f_c the cut-off frequency and ξ denotes the damping ratio.

$$\frac{V_o}{V_I} = \frac{S^2}{S^2 + 2\xi(2\pi f_c)S + (2\pi f_c)^2} \quad (2)$$

2.4 ANN Classification

Fig. 7 shows the pre-processed current signal obtained by the data acquisition module when the brushed DC motor start. The processed current signal has periodic ripple of obvious features that can be illustrated in Fig. 8. Each ripple begins with sharp raise to α, and continued with a sharp fall ending at t = β. The ripple then followed by a raise to ε and drop back at t = β + γ.

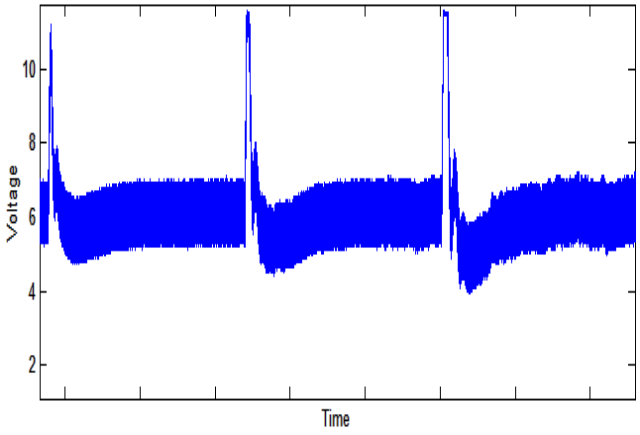

Fig. 7 Signal acquired by the data acquisition card

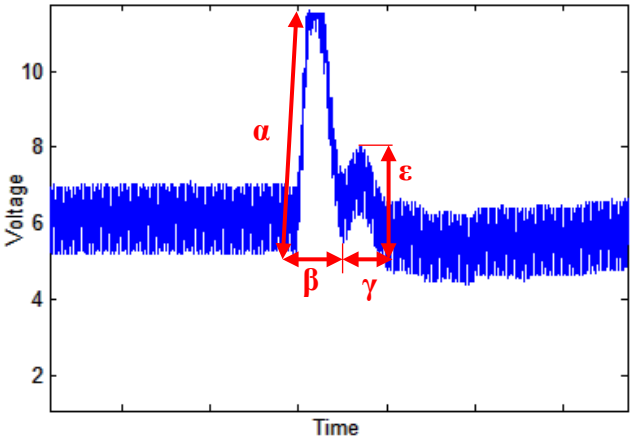

Fig. 8 Enlargement of the signal acquired by the data acquisition card

In any design, training a set of data in a neural network requires preprocessing step as illustrated in Fig. 9.

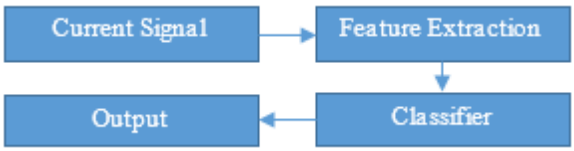

Fig. 9 ANN Flow

Preprocessing stage includes the feature extraction stage. In this research, the features are extracted from the train of signal acquired from the data acquisition card. The data contains signals that has periodic ripples which are extracted out to be as used as input to the classifier. The input data are α, ε, β and γ. The output are detected and non- detected signals In this research, backpropagation algorithm is used as the neural network classifier. A well trained neural network will generate reasonable answers when the network is introduced with new set of data that is not included in the training and validation set. A general ANN will have three layers which are input layer, hidden layer and output layer. The network is trained until it reaches the smallest Mean Squared Error (MSE). Early stopping criteria is added to avoid the network from being overtrained which may lead to underfitting or overfitting data. The data that is fed into the network is divided randomly into three parts which are training (70%), testing (20%) and validation (10%) data. The training data is used to compute the gradient and update the network weight and bias. The validation set data is related with the stopping criteria and finally the testing set is used to test the network performance. One of the most important parameter in a neural network is the number of hidden neuron. Equation (3) represents the formula to determine the number of hidden neurons.

$$N_h = \sqrt{N_i N_o} \quad (3)$$

Thus, the number of hidden neuron for this network is 3
The network is trained based on several defined parameters. These parameters are obtained after several trial and error method. Table 1 shows the parameter setting for the network. The total number of samples are 1500 which includes the true and false data.

Table 1: ANN parameter setting

Number of Hidden Layer	1
Number of Input Neuron	4
Number of Output Neuron	2
Number of Hidden Neuron	3
Training Algorithm	trainscg
Transfer Function	tansig

3. Results and Discussion

In this section, the complete system is tested for two scenarios: uncontrolled motor start-up (full power and no pulse width modulation) and controlled motor start-up (pulse width modulation applied to limit the starting torque). The predicted speed results are then compared to the optical encoder. In this test, the average error (instantaneous speed error) and deviation error (positional error), with respect to real speed and position, were obtained. Both deviation and average errors are shown in relative value (in percent).

3.1 Neural Network Analysis

This section discusses the result of the network training and testing. Fig. 10 displays the network performance. From this figure, it can be seen that the network was trained until it reaches the performance goal of 0.01 with 36 epoch. The validation and curve shows that the MSE error decreases and no over-fitting or under fitting found.

IJISET - International Journal of Innovative Science, Engineering & Technology, Vol. 3 Issue 6, June 2016
ISSN (Online) 2348 – 7968 | Impact Factor (2015) - 4.332
www.ijiset.com

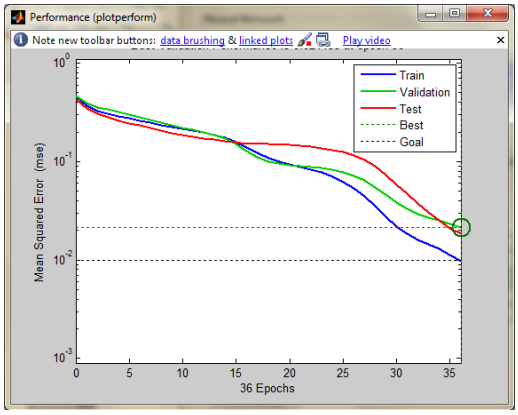

Fig. 10 ANN performance

Figure 11 shows the regression plot. From this graph, the all the training, testing and validation data fits close to the curve.

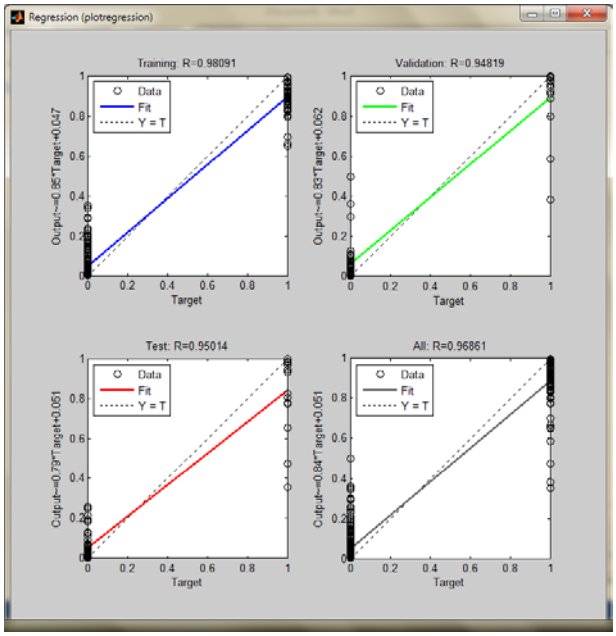

Fig. 11 ANN regression plot

3.2 Uncontrolled Start-up

The uncontrolled start-up experiment is run 40 times for each applied voltage starting from minimal operating voltage (10V) to maximum operating voltage (24V). The power is supplied directly from a voltage controlled power supply (Current limit: 16A) to the driver module. The brushed DC motor start-up duration of each voltage test is different and is defined from 0% to 90% of the steady-state speed. The experimental result is tabulated in Table 2 and plotted in Fig. 12. The average error and deviation graph in Fig. 12 shows an uptrend as the acceleration or torque increases in an uncontrolled starting.

Table 2: Speed and position measurement errors for uncontrolled start-up

Voltage	*Average Error (%)*	*Deviation (%)*
10	0.18	0.22
12	0.21	0.26
14	0.23	0.28
16	0.24	0.29
18	0.33	0.42
20	0.37	0.51
22	0.39	0.53
24	0.41	0.55

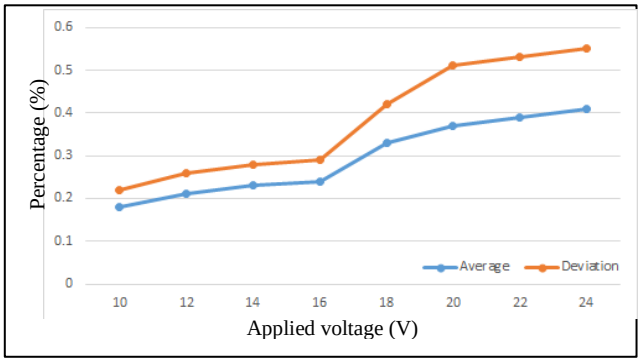

Fig. 12 Average error and deviation for uncontrolled start-up.

3.3 Controlled Start-up

The controlled start-up experiment is run 40 times for each applied voltage. The power is supplied directly from a voltage controlled power supply (Current limit: 16A) to the driver module. All the iterations of the experiment are driven with a pulse width modulation ramp from 20% to 100% duty cycle in 1 second. The brushed DC motor start-up duration of each voltage test is different and is defined from 0% to 90% of the steady-state speed.

The experimental result is tabulated in Table 3 and plotted in Fig. 13. The average error and deviation graph in Fig. 13 shows that controlled starting with pulse width modulation ramp will result in lowered error when the proposed method is implemented. However, the percentage of both average error and deviation showed an uptrend as the supply voltage increases.

Table 3: Speed and position measurement errors for controlled start-up

Voltage	*Average Error (%)*	*Deviation (%)*

10	0.05	0.08
12	0.06	0.09
14	0.06	0.09
16	0.08	0.10
18	0.08	0.11
20	0.08	0.11
22	0.09	0.13
24	0.10	0.15

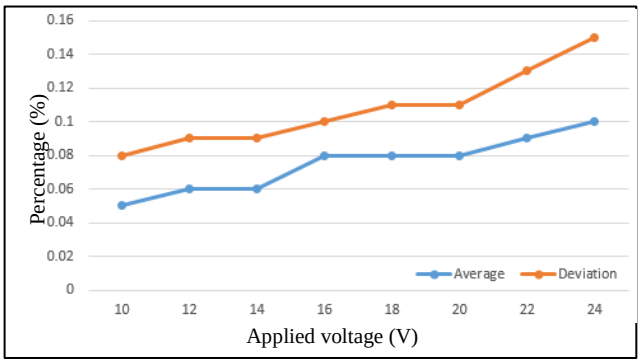

Fig. 13 Average error and deviation for controlled start-up.

4. Conclusions

This paper has presented a new sensorless method for estimating the speed of brushed dc motors at starting up. The method uses sensorless techniques based on the current ripple component at starting-up. The method employs active filters and amplifiers to normalize and extract the useful features of the current signal for digital processing. To enable rotor speed measurement and estimation, artificial neural network based pattern recognition technique is employed to detect the periodic current ripple generated in brushed dc motor during commutation. The artificial neural network is trained based on the heights and widths of the ripple pulses. Finally, the trained network can recognize the current ripple pulses for the system to count in order to estimate the position and speed of the brushed DC motor. The experimental results were obtained to validate the proposed method, showing that the method works in a wide range of starting up speeds and in different operating conditions, such as abrupt starting and ramp start up.

Acknowledgments

Authors would like to thank Universiti Malaysia Sabah for the research grant SBK0152-TK-2014 and Artificial Intelligence Research Unit (AiRU).

References

[1] D. Ishak and A. H. Abu Hassan, "Analytical modeling of permanent magnet excited brushed DC motor for low-cost applications," in Proceeding of the 5th International Symposium on Mechatronics and its Applications, Amman, 2008.

[2] G. M. G., F. G. and C. A., "A Sensorless PMDC Motor Speed Controller with a Logical Overcurrent Protection," Journal of Power Electronics, vol. 13, no. 3, pp. 381-389, 2013.

[3] G. G. Rigatos and P. Siano, "Sensorless Control of Electric Motors with Kalman Filters: Applications to Robotic and Industrial Systems," International Journal of Advanced Robotic Systems, vol. 8, no. 6, pp. 62-80, 2011.

[4] W. C., W. B., G. M., K. J. and S. U., "A Virtual Rapid Analysis Model for DC Motors with Single Tooth Windings," in International Conference on Electrical Machines (ICEM), Berlin, 2014.

[5] A. E., N. G. A. and K. A., "Sensorless Speed/Position Control of Brushed DC Motor," in International Aegean Conference on Electrical Machines and Power Electronics, Bodrum, 2007.

[6] J. B. Nottelmann, "Sensor-less Rotation Counting in Brush Commutated DC motors," IDEAdvance Ltd., US, 2010.

[7] K. C. Agees and N. N. Kesavan, "Multi-Objective PI Controller Design with an Application to Speed Control of Permanent Magnet DC Motor Drives," in Proceedings of International Conference on Signal Processing, Communication, Computing and Networking Technologies, Thuckafay, 2011.

[8] R. Pj and D. Kumar, "Sensorless speed measurement for brushed DC motors," IET Power Electronics, vol. 8, no. 11, pp. 2223-2228, 2015.

[9] J. M. Kneževic, "Low-Cost Low-Resolution Sensorless Positioning of DC Motor Drives for Vehicle Auxiliary Applications," IEEE Transactions on vehicular technology, vol. 62, no. 9, pp. 4328-4335, 2013.

[10] C.-T. Chi and S.-A. Yin, "Speed Measurement of a General DC Brushed Motor Based on Sensorless Method," in Conference on Power & Energy, Ho Chi Minh, 2012.

[11] E. Vázquez-Sánchez, J. Gómez-Gil, J. C. Gamazo-Real and J. F. Díez-Higuera, "A New Method for Sensorless Estimation of the Speed and Position in Brushed DC Motors Using Support Vector Machines," IEEE Transactions on Industrial Electronics, vol. 59, no. 3, pp. 1397-1408, 2012.

[12] Beham, M. P. & Roomi, M. M. 2013. A Review on Face Recognition Methods. International Journal of Pattern

Recognition and Artificial Intelligence. 27(4):13560051-135600535.

[13] Krenker, A., Bester, J. & Kos, A. 2011. Introduction to the Artificial Neural Networks. Artificial Neural Network-Methodological Advances and Biomedical Applications. Croatia: Intech. 1-17.

[14] M. Hajek. 2005. Neural Networks. http://www.cs.ukzn.ac.za/notes/NeuralNetworks2005.pdf.1-114